Plasma production of nanocrystalline silicon particles and polymorphous silicon thin films for large-area electronic devices*

Pere Roca i Cabarrocas‡, Anna Fontcuberta i Morral, Sarra Lebib, and Yves Poissant

Laboratoire de Physique des Interfaces et des Couches Minces (UMR 7647 – CNRS) Ecole Polytechnique, 91128 Palaiseau Cedex, France

Abstract: Powder formation in silane plasmas has been considered as a technology drawback because it might lead to the formation of macroscopic defects in the deposited layers. Here we summarize our recent efforts in controlling the formation of powder precursors, in particular, nanocrystalline silicon particles, aiming at their incorporation in the films. Indeed, the incorporation of clusters and crystallites along with SiH_x radicals allows production of polymorphous silicon films with improved structure and transport properties with respect to standard amorphous silicon films.

INTRODUCTION

Large-area electronics is an expanding field which, like microelectronics, is based on plasma processes, particularly on the use of capacitively coupled radio-frequency glow discharge reactors, nowadays capable of a uniform deposition on glass plates with sizes above 1 m^2. Silane plasmas have been widely studied with respect to the plasma processes (primary and secondary reactions), the plasma/surface interactions, the film growth mechanisms, and the hydrogenated amorphous silicon (a-Si:H) properties (Fig. 1). As a result, there is a large consensus on SiH_3 being the "good radical" [1] to produce a low-defect density a-Si:H (of the order of 10^{15}–10^{16} defects per cm^3, i.e., only one defect over 10^6–10^7 atoms). Thus, the ingredients for a low-defect density material are SiH_3 radicals and a substrate temperature high enough (150–250 °C) to provide mobility to the radicals on the surface and promote cross-linking reactions leading to the elimination of excess hydrogen, to end up with typically 10 % atomic hydrogen in the film [2].

Such amorphous silicon thin films (a-Si:H) are the basis of a large number of devices. Indeed, despite the disordered nature of this semiconductor, its electronic properties are good enough to produce electronic devices such as solar cells, thin-film transistors for active matrix liquid crystal displays, photo and particle detectors, etc. [3]. Nevertheless, further improvement of the performances of these devices will require a reduction in the density of defects of the material—related to a reduction of its disorder—as well as to enhance its stability. For example, a-Si:H solar cells suffer from the creation of metastable defects upon recombination of photogenerated electrons and holes, which results in a 20 to 30 % reduction in the cell efficiency when submitted to prolonged exposure to light.

Besides the improvement of the material properties, cost reduction is another key point when transferring the research results into production. This often implies increasing the deposition rate, which

can be achieved by increasing the RF power, the pressure in the reactor, etc. (see Fig. 1). However, the increase in deposition rate from typically 0.1 nm/s up to a few 10 nm/s generally results in the formation of powder, and eventually in the deterioration of the a-Si:H properties. As a matter of fact, low-defect density a-Si:H films can be deposited at high rates under powder conditions [4]. Nevertheless, powders have a negative connotation, and the subject of dusty or complex plasmas [5] has experienced a large development in the last decade. This brings us to the topic of this paper: not the dust itself, but the dust precursors. To begin with, we were interested to understand powder formation in order to avoid it or to manage it, as powder is associated with the achievement of high deposition rates. From the study of square-wave modulated discharges we could observe the formation of silicon nanocrystals (powder precursors) even at room temperature [6,7]. This finding completely changed our strategy and pushed us to work under plasma conditions at the onset of powder formation [4]. The aim is to produce nanostructured silicon thin films under plasma conditions where silicon clusters, nanoparticles and crystallites are formed. Among these nanostructured materials, we have recently focused on polymorphous silicon (pm-Si:H), which shares the high optical absorption of a-Si:H while having improved electronic and transport properties [8,9].

We here summarize our recent work on the synthesis and the characterization of both nanocrystalline silicon particles and polymorphous silicon thin films.
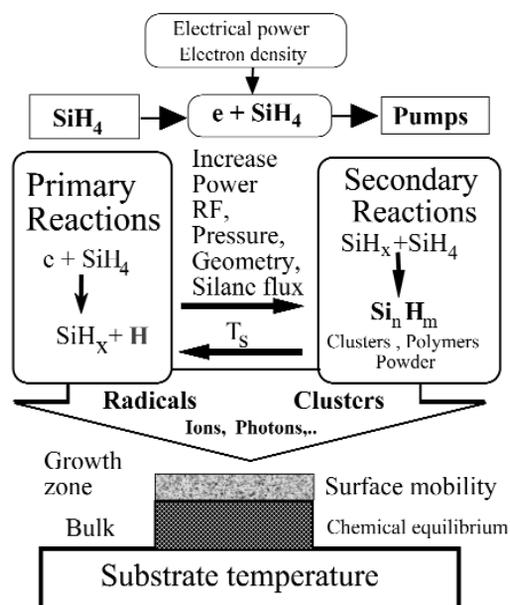

Fig. 1 Schematic representation of the processes involved in amorphous silicon deposition.

EXPERIMENTS

Nanocrystalline silicon particles, polymorphous silicon films, and solar cells were produced using the standard RF glow discharge technique [10] from the decomposition of silane highly diluted in hydrogen. Moreover, the temperature of the substrate holder and that of the RF electrode, as well as the inter-electrode distance could be varied in order to modify the temperature gradient between the electrodes. The samples were co-deposited on different substrates to enhance comparisons between the various characterization techniques. Cavity ring down measurements were performed to detect the presence of

clusters and to evaluate their concentration [11]. Growth studies were performed using *in situ* ellipsometry measurements, also used to characterize the optical properties and the structure of the films. A large set of experimental techniques has been used for the characterization of the electronic and transport properties of the pm-Si:H films. In particular, high-resolution transmission electron microscopy (HRTEM) was used to demonstrate the presence of crystallites [12]. The hydrogen-related structure was studied by infrared transmission and hydrogen evolution experiments. Finally, solar cells with pm-Si:H absorber i-layers and having standard p-type a-SiC:H layer and n-type a-Si:H layer were deposited on tin oxide-coated glass substrates. The cells were subjected to accelerated light-soaking tests in order to compare the evolution of their properties to those of standard a-Si:H solar cells [13].

RESULTS AND DISCUSSION

Figure 2 gives a schematic description of the different phases involved in the process of powder formation. While these phases have been studied in detail elsewhere [5,14], here we want to emphasize on the nature of the material produced at the different stages. Powders are easily detected and characterized both in the plasma as well as by *ex situ* techniques. As shown in Fig. 2, powders often display a cauliflower structure, which images the agglomeration phase. After agglomeration, the powders are negatively charged and trapped in the discharge. This is the reason why they do not contribute to deposition. Moreover, as they present a large surface on which the most reactive radicals (SiH_2, SiH) can be lost, the presence of powders in the discharge can be viewed as a way to select SiH_3 radicals and produce high-quality a-Si:H films even at high deposition rates. Of course, the radicals and clusters leading to powders are lost for deposition, and care has to be taken to avoid powders from falling onto the substrate when the discharge is switched off. Thus, powder management has been a subject of interest in the last few years to take advantage of the positive aspects of powders while avoiding the negative ones.

Along these lines, the study of the initial stage of powder formation has been addressed as a way to control powder formation. An elegant way to stop the process before the coagulation phase is the use of square-wave modulated discharges [15,16]. By turning off the plasma before the onset of powder formation, one can collect on the substrate the precursors of powders. Figure 2 gives an example of such
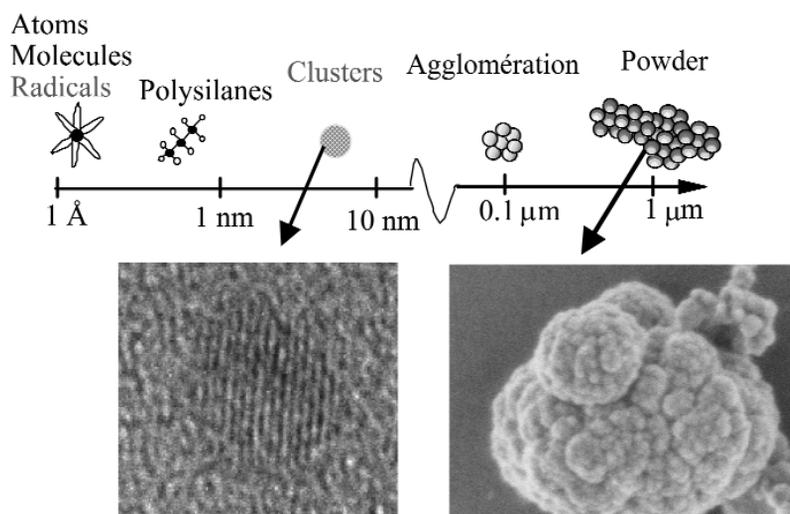

Fig. 2 Schematic illustration of the genesis of powder formation in silane plasmas along with a scanning electron micrograph of a large powder and a high-resolution electron transmission electron microscopy of a nanocrystalline silicon particle.

studies in which a nanocrystalline silicon particle was collected from a 250-ms silane argon discharge at room temperature [17]. This result has strong consequences in the field of low-pressure plasmas and nanostructured materials as it demonstrates that nanocrystalline silicon particles can be produced even at room temperature. Of course, the obtaining of nanocrystalline silicon particles opens new questions: Why are they crystalline?; What is their size distribution?; and How to deposit them on a substrate?

The crystalline structure of the nanoparticles could be either a consequence of their growth process, or an artifact of the characterization technique, such as the crystallization induced by the electron beam. As a matter of fact, the produced particles are not always crystalline [18], and Fig. 3a gives an example of amorphous silicon particles produced in a silane plasma. While in the case of small crystallites, some doubts may remain about their structure before characterization (crystallization), the large polycrystalline silicon powders shown in Fig. 3b provide a clear proof of the possibility to produce crystalline silicon particles in silane discharges commonly used for a-Si:H deposition.

As a result, our objective in the study of dusty plasmas is to favor the production of ordered clusters and crystalline silicon particles, and to incorporate them into the a-Si:H matrix. We emphasize on nanocrystalline silicon particles and/or clusters because HRTEM measurements do not allow to clearly distinguish small (1–2 nm) crystalline silicon particles in an a-Si:H matrix. Thus, along with the detected 3–5-nm crystalline silicon particles, a larger concentration of smaller ordered clusters and crystallites can contribute to the deposition and have a strong effect on the material properties, despite the fact that we are unable to distinguish them from matrix.

While square-wave modulated discharges offer a way to select the size of nanoparticles, we have been focusing on continuous plasmas under conditions close to powder formation. Indeed, nanometer-size particles experience charge fluctuations, allowing them to escape from the plasma [6]. Different process parameters: pressure, power, dilution, and temperature as indicated in Fig. 1 can be varied to move the plasma conditions to the powder regime. Figure 4 shows the evolution of the deposition rate as a function of pressure in a 3 % silane in hydrogen discharge at 250 °C under an RF power of 80 mW/cm^2. Three zones can be distinguished. In the low-pressure range, the produced material is microcrystalline silicon, resulting from surface and subsurface reactions of the impinging atomic hydrogen, SiH$_x$ radicals, and ions [19]. At high pressure, powders are formed in the reactor, and the deposition rate increases owing to a better coupling of the RF power to the plasma. However, as more powder accumulates in the plasma, it will trap radicals, and eventually the deposition rate will decrease [4].
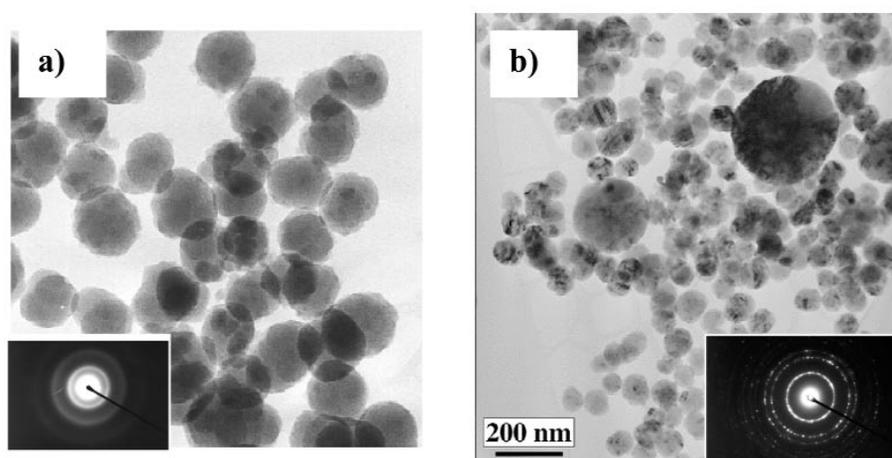

Fig. 3 TEM micrographs of amorphous (a) and crystalline (b) silicon particles. The amorphous or crystalline structure is clearly evidenced by the electron diffraction patterns shown in the insets.

Also, as shown in Fig. 2, the formation of powder occurs via the agglomeration of clusters and crystallites, which will not contribute to deposition. Then, the material produced at high pressure, under powder conditions, is a-Si:H. In the intermediate pressure range, the concentration of crystallites and clusters is assumed to increase with pressure. Indeed, under continuous plasma the transition from a pristine to a powder discharge as detected by Mie scattering is sharp [6]. However, for agglomeration to occur the particles cannot be negative so that they can contribute to deposition provided their transit time from the plasma to the substrate is shorter than the charging time.

Interestingly enough, the increase in deposition rate shown in Fig. 4 is correlated with an improvement on the electronic properties of the films, which show an optimum in the pressure range of 1200 up to 1800 mTorr, depending on temperature, dilution, RF power, etc. (i.e., on how fast powder forms in the reactor) [8].

Of course, the question is what is the reason for the observed improvement of transport properties. Different hypothesis can be formulated: (i) decrease of ion energy, (ii) change in the nature of radicals, and (iii) contribution of clusters and or crystallites to deposition.

Increasing pressure will reduce the energy of the ions reaching the substrate and thus create fewer defects on the growing film, as observed in microcrystalline silicon. However, the contributions of ions to the growth of pm-Si:H films is much higher than in the case of a-Si:H deposition, and it is not clear why there should be an optimum pressure [19]. On the other hand, the change in the nature of the radicals with pressure seems natural and could explain the improvement in the material properties, but again it is not clear why there should be an optimum, and the hypothesis is not consistent with the increase in deposition rate.

The contribution of clusters to the deposition seems a reasonable way to explain the increase in deposition rate in the intermediate pressure range. Moreover, if clusters contribute to deposition, one could expect them to affect the structure of the material, in particular the hydrogen-related structure. We have shown in previous studies that besides the 2000 cm^{-1} and the 2090 cm^{-1} bands, associated to isolated Si–H bonds and hydrogen bonded at the surface of cavities in a-Si:H- pm-Si:H films, are charac-
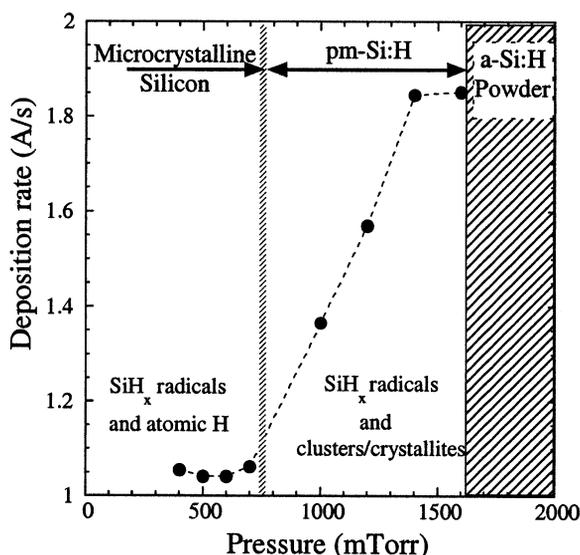

Fig. 4 Deposition rate as function of pressure in a 3 % silane in hydrogen mixture at 250 °C under an RF power of 80 mW/cm^2. As pressure increases the deposited material changes from microcrystalline silicon [4], to polymorphous silicon in the intermediate pressure range, and amorphous silicon at high pressure where powders are formed by the agglomeration of clusters (see Fig. 2). The line is provided as a guide to the eyes.

terized by the presence of a peak at 2030 cm^{-1} in their infrared absorption, related to hydrogen bonded at the surface of clusters or crystallites [20]. Figure 5 shows the evolution of the integrated absorption of the 2030 cm^{-1} band along with that of the 2090 cm^{-1}. In the low-pressure regime, the band at 2090 cm^{-1} corresponding to hydrogen bonded in microcrystalline silicon is dominant, then vanishes in the pm-Si:H deposition conditions and increases again at high pressure, under powder conditions where a-Si:H is obtained. The evolution of the 2030 cm^{-1} band, characteristic of polymorphous silicon films shows a clear optimum, corresponding to a maximum flux of clusters to the substrate, before the onset of powder formation. Note that the optimum in the 2030 cm^{-1} band corresponds to optimized deposition conditions for the electronic properties [8] and to the improvement in the order of the material [21]. The increased order is in our opinion the reason for the improvement in the transport properties that allow to increase the efficiency and the stability of p-i-n solar cells [13]. In this sense, polymorphous silicon appears as an alternative to further improve the performances, reduce costs, and make a-Si:H-like technology more competitive.

Further optimization of pm-Si:H properties would require a better understanding of the plasma chemistry leading to clusters and crystallites [22], as well as from more refined diagnostic techniques. Indeed, the detection of nanometer-size silicon particles in the plasma remains a challenging issue. Some studies have focused on this issue and advanced techniques [5] such as laser-induced particle explosion, photon counting, and cavity ring down (CRD) have been developed to get an information on the "cluster phase" (Fig. 2). Here we will focus on cavity ring down measurements combined with *in situ* ellipsometry growth studies that have revealed the importance of nanoparticles on polymorphous silicon deposition [23]. Indeed, thermophoresis and gas drag appear to be the main forces acting on nanometer-size particles. In a series of experiments where the substrate temperature, the RF electrode temperature and the inter-electrode distance could be independently changed, the structure of the films was monitored by spectroscopic ellipsometry.

Table 1 shows the structure of the deposited films as a function of the thermal gradient between the two electrodes. We can see that when the gradient is higher than 50 °C/cm (the nanoparticles are
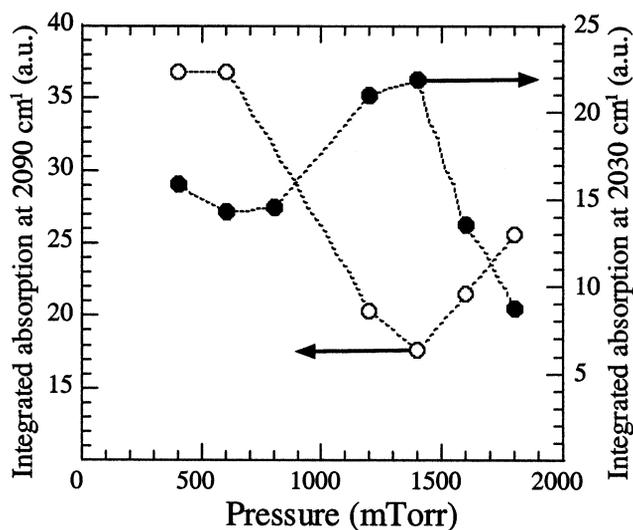

Fig. 5 Effect of the pressure on the 2090 cm^{-1} infrared absorption band associated to hydrogen bonded at the surface of crystalline silicon and voids in amorphous silicon, and of the band 2030 cm^{-1}, characteristic of polymorphous silicon films and indicating the presence of hydrogen bonded at the surface of clusters and nanocrystalline silicon particles. The lines are provided as a guide to the eyes.

Table 1 Structure as a function of the thermal gradient. Silicon thin films produced under constant plasma conditions: 3 sccm of silane plus 140 sccm of hydrogen under a total pressure of 133 Pa and an RF power of 100 mW/cm^2. Note that the structure of the films is governed by the thermal gradient between the electrodes.

Sample	Temperature RF/PS($^\circ$C)	Inter-electrode distance d(cm)	$(T_{RF}-T_s)/d$ ($^\circ$C/cm)	Material
90317C	200/150	2	+25	**pm-Si:H**
90325B	150/150	2	0	**pm-Si:H**
90317B	100/150	2	–25	**pm-Si:H**
90318A	50/150	2	–50	**µc-Si:H**
91012A	50/150	2.7	–39	**pm-Si:H**
91111A	50/250	2.7	–74	**µc-Si:H**

pushed away from the substrate holder) the material is microcrystalline, while when the powders are attracted to the substrate, the material is polymorphous. The analysis of the concentration of particles in the plasma under pm-Si:H deposition conditions requires highly sensitive techniques such as cavity ring down [24]. In this way, we have been able to detect the transition from a cluster plasma to a powder discharge and to control the concentration of particles in the plasma [11], provided a few hypothesis are made. Figure 6 shows the time evolution of the extinction coefficient deduced from CRD measurements for different inter-electrode distances. As this distance increases, secondary reactions are favored (Fig. 1) and lead to the formation of powders. We can see that as the inter-electrode distance increases the extinction coefficient also increases until it goes through a complete change for an inter-electrode distance above 4.3 cm. If we assume that the extinction is produced by 2-nm-diameter crystalline silicon particles, then we can calculate their concentration in the plasma [11]. Thus, increasing the inter-electrode distance from 2.8 to 4.3 cm allows us to increase the concentration of particles by a factor of 5. We note that up to a distance of 4.3 cm the concentration remains lower than the threshold for agglomeration, estimated at about 10^{11} cm^{-3} [25], and, thus, at this pressure the produced particles can contribute to the deposition of pm-Si:H films. Then, the improvement of the electronic properties
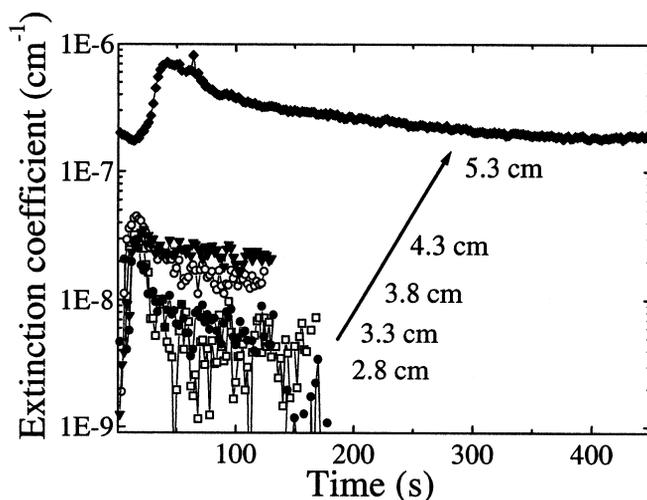

Fig. 6 Evolution of the absorption coefficient in a 4.5 % silane in hydrogen discharge with a total pressure of 1000 mTorr and RF power of 7 W. The substrate and the RF electrode temperature were both fixed at 250 °C. The inter-electrode distance was varied in order to promote secondary reactions and powder formation.

of the pm-Si:H films with pressure, inter-electrode distance, etc., can be understood as an increase of the concentration of clusters and crystallites contributing to deposition.

Further studies are necessary to better control the size and concentration of clusters/crystallites in the plasma. The better understanding of the plasma chemistry leading to the formation of nanocrystalline silicon particles, the development of diagnostic techniques to control their size and concentration, and the development of methods to control their deposition on the substrate, constitute a tremendous challenge for the plasma community for the next few years.

CONCLUSION

As a conclusion, pioneering studies of powder formation in silane plasmas, aiming to suppress its formation, have been diverted towards the production of nanocrystalline silicon particles. When deposited along with silane radicals, nanostructured materials such as polymorphous silicon are obtained. The improved electronic properties of this material make it a challenging alternative to a-Si:H in the field of large-area electronics. Moreover, the precise control of the size and concentration of nanocrystalline silicon particles in the plasma should open the way to the nanoelectronics field in which the plasma produced nanocrystallites can be passivated, coated, etc., and finally incorporated in devices such as nonvolatile memories, single-electron transistors, and so on.

ACKNOWLEDGMENTS

REFERENCES

1. G. Ganguly and A. Matsuda. *Phys. Rev. B*. **47**, 3661 (1993).
2. R. A. Street. *Hydrogenated Amorphous Silicon*, Cambridge University Press, Cambridge (1991).
3. See, for example, the *Proceedings of the Symposium on Thin Films for Large Area Electronics*, E-MRS 2000 published in *Thin Solid Films*, Vol. **383** (2001).
4. P. Roca i Cabarrocas. *J. Non-Cryst. Solids* **266–269**, 31 (2000) and references therein.
5. For a recent review, see *Dusty Plasmas*, A. Bouchoule (Ed.), John Wiley, England (1999).
6. P. Roca i Cabarrocas, P. Gay, A. Hadjadj. *J. Vac. Sci. Technol. A* **14**, 655 (1996).
7. P. Roca i Cabarrocas. *MRS Symp. Proc*. **507**, 855 (1998).
8. R. Butté, R. Meaudre, M. Meaudre, S. Vignoli, C. Longeaud, J. P. Kleider, P. Roca i Cabarrocas. *Philos. Mag. B* **79**, 1079 (1999).
9. J. P. Kleider, C. Longeaud, M. Gauthier, M. Meaudre, R. Meaudre, R. Butté, S. Vignoli, P. Roca i Cabarrocas. *Appl. Pys. Lett.* **75**, 3351 (1999).
10. P. Roca i Cabarrocas, J. B. Chévrier, J. Huc, A. Lloret, J. Y. Parey, J. P. M. Schmitt. *J. Vac. Sci. Technol. A* **9**, 2331 (1991).
11. A. Fontcuberta i Morral, F. Grangeon, P. Roca i Cabarrocas. To be published.
12. A. Fontcuberta i Morral, R. Brenot, E. A. G. Hamers, R. Vanderhaghen, P. Roca i Cabarrocas. *J. Non-Cryst. Solids* **266–269**, 48 (2000).
13. P. Roca i Cabarrocas, P. St'ahel, S. Hamma Y. Poissant, *Proc. 2nd World Conference on Photovoltaic Solar Energy Conversion*, Vienna, Austria (1998), p. 355. J. Schmid, H. A. Ossenbrink, P. Helm, H. Ehmann, E. D. Dunlop (Eds.), Report EUR 18656 EN, Joint Research Centre, European Commission.
14. Ch. Hollenstein. *Plasma Phys. Control. Fusion* **42**, R93 (2000).
15. A. Howling, J.-L. Dorier, Ch. Hollenstein. *Appl. Phys. Lett*. **62**, 1341 (1993).

16. L. Boufendi, A. Plain, J. Ph. Blondeau, A. Bouchoule, C. Laure, M. Toogood. *Appl. Phys. Lett*. **60**, 169 (1992).
17. J. Costa, P. Roura, P. Roca i Cabarrocas, G. Viera, E. Bertran. *MRS Symp. Proc*. **507**, 499 (1998).
18. J. Costa, G. Sardin, J. Campmany, J. L. Andujar, A. Canillas, E. Bertran. *MRS Symp. Proc*. **297**, 1031(1993).
19. E. A. G. Hamers, A. Fontcuberta i Morral, C. Niikura, R. Brenot, P. Roca i Cabarrocas. *J. Appl. Phys*. **88**, 3674 (2000).
20. P. Roca i Cabarrocas, S. Hamma, S. N. Sharma, J. Costa, E. Bertran. *J. Non-Cryst. Solids* **227–230**, 871 (1998).
21. A. Fontcuberta i Morral and P. Roca i Cabarrocas. *J. Non-Cryst. Solids* **299–302** (2002). To be published.
22. M. T. Swihart and S. L. Girshick. *J. Phys. Chem. B* **103**, 64 (1999).
23. A. Fontcuberta i Morral and P. Roca i Cabarrocas. *Thin Solid Films* **383**, 161 (2001).
24. F. Grangeon, C. Monard, J.-L. Dorier, A. A. Howling, Ch. Hollenstein, D. Romanini, N. Sadeghi. *Plasma Sources Sci. Technol*. **8**, 448 (1994).
25. A. A. Fridman, L. Bufendi, T. Hbid, B. V. Potapkin, A. Bouchoule. *J. Appl. Phys*. **79**, 1303 (1996).